

Adaptive PI Control of STATCOM for Voltage Regulation

Yao Xu, *Student Member, IEEE*, and Fangxing Li, *Senior Member, IEEE*

Abstract—STATCOM can provide fast and efficient reactive power support to maintain power system voltage stability. In the literature, various STATCOM control methods have been discussed including many applications of proportional-integral (PI) controllers. However, these previous works obtain the PI gains via a trial-and-error approach or extensive studies with a tradeoff of performance and applicability. Hence, control parameters for the optimal performance at a given operating point may not be effective at a different operating point. This paper proposes a new control model based on adaptive PI control, which can self-adjust the control gains during a disturbance such that the performance always matches a desired response, regardless of the change of operating condition. Since the adjustment is autonomous, this gives the plug-and-play capability for STATCOM operation. In the simulation test, the adaptive PI control shows consistent excellence under various operating conditions, such as different initial control gains, different load levels, change of transmission network, consecutive disturbances, and a severe disturbance. In contrast, the conventional STATCOM control with tuned, fixed PI gains usually perform fine in the original system, but may not perform as efficient as the proposed control method when there is a change of system conditions.

Index Terms—Adaptive control, plug and play, proportional-integral (PI) control, reactive power compensation, STATCOM, voltage stability.

I. INTRODUCTION

VOLTAGE stability is a critical consideration in improving the security and reliability of power systems. The static compensator (STATCOM), a popular device for reactive power control based on gate turnoff (GTO) thyristors, has gained much interest in the last decade for improving power system stability [1].

In the past, various control methods have been proposed for STATCOM control. References [2]–[9] mainly focus on the control design rather than exploring how to set proportional-integral (PI) control gains. In many STATCOM models,

the control logic is implemented with the PI controllers. The control parameters or gains play a key factor in STATCOM performance. Presently, few studies have been carried out in the control parameter settings. In [10]–[12], the PI controller gains are designed in a case-by-case study or trial-and-error approach with tradeoffs in performance and efficiency. Generally speaking, it is not feasible for utility engineers to perform trial-and-error studies to find suitable parameters when a new STATCOM is connected to a system. Further, even if the control gains have been tuned to fit the projected scenarios, performance may be disappointing when a considerable change of the system conditions occurs, such as when a line is upgraded or retires from service [13], [14]. The situation can be even worse if such transmission topology change is due to a contingency. Thus, the STATCOM control system may not perform well when mostly needed.

A few, but limited previous works in the literature discussed the STATCOM PI controller gains in order to better enhance voltage stability and to avoid time-consuming tuning. For instance, in [15]–[17], linear optimal controls based on the linear quadratic regular (LQR) control are proposed. This control depends on the designer's experience to obtain optimal parameters. In [18], a new STATCOM state feedback design is introduced based on a zero set concept. Similar to [15]–[17], the final gains of the STATCOM state feedback controller still depend on the designer's choice. In [19]–[21], a fuzzy PI control method is proposed to tune PI controller gains. However, it is still up to the designer to choose the actual, deterministic gains. In [22], the population-based search technique is applied to tune controller gains. However, this method usually needs a long running time to calculate the controller gains. A tradeoff of performance and the variety of operation conditions still has to be made during the designer's decision-making process. Thus, highly efficient results may not be always achievable under a specific operating condition.

Different from these previous works, the motivation of this paper is to propose a control method that can ensure a quick and consistent desired response when the system operation condition varies. In other words, the change of the external condition will not have a negative impact, such as slower response, overshoot, or even instability to the performance.

Based on this fundamental motivation, an adaptive PI control of STATCOM for voltage regulation is presented in this paper. With this adaptive PI control method, the PI control parameters can be self-adjusted automatically and dynamically under different disturbances in a power system. When a disturbance occurs in the system, the PI control parameters for STATCOM can be computed automatically in every sampling time period

Manuscript received February 20, 2012; revised December 21, 2012, August 16, 2013, and October 29, 2013; accepted November 07, 2013. Date of publication February 14, 2014; date of current version May 20, 2014. This work was supported in part by Stanford University—Global Climate and Energy Project (GCEP). This work also made use of CURENT Shared Facilities supported by the National Science Foundation (NSF) and DOE under NSF Award Number EEC-1041877 and the CURENT Industry Partnership Program. Paper no. TPWRD-00172-2012.

The authors are with the Department of Electrical Engineering and Computer Science, The University of Tennessee (UT), Knoxville, TN 37996 USA (e-mail: flf16@utk.edu).

Color versions of one or more of the figures in this paper are available online at <http://ieeexplore.ieee.org>.

Digital Object Identifier 10.1109/TPWRD.2013.2291576

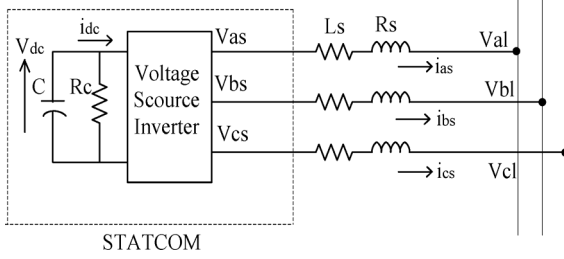


Fig. 1. Equivalent circuit of STATCOM.

and can be adjusted in real time to track the reference voltage. Different from other control methods, this method will not be affected by the initial gain settings, changes of system conditions, and the limits of human experience and judgment. This will make the STATCOM a “plug-and-play” device. In addition, this research work demonstrates fast, dynamic performance of the STATCOM in various operating conditions.

This paper is organized as follows. Section II illustrates the system configuration and STATCOM dynamic model. Section III presents the adaptive PI control method with an algorithm flowchart. Section IV compares the adaptive PI control methods with the traditional PI control, and presents the simulation results. Finally, Section V concludes this paper.

II. STATCOM MODEL AND CONTROL

A. System Configuration

The equivalent circuit of the STATCOM is shown in Fig. 1. In this power system, the resistance R_s in series with the voltage-source inverter represents the sum of the transformer winding resistance losses and the inverter conduction losses. The inductance L_s represents the leakage inductance of the transformer. The resistance R_c in shunt with the capacitor C represents the sum of the switching losses of the inverter and the power losses in the capacitor. In Fig. 1, V_{as} , V_{bs} , and V_{cs} are the three-phase STATCOM output voltages; V_{al} , V_{bl} , and V_{cl} are the three-phase bus voltages; and i_{as} , i_{bs} , and i_{cs} are the three-phase STATCOM output currents [15], [23].

B. STATCOM Dynamic Model

The three-phase mathematical expressions of the STATCOM can be written in the following form [15], [23]:

$$L_s \frac{di_{as}}{dt} = -R_s i_{as} + V_{as} - V_{al} \quad (1)$$

$$L_s \frac{di_{bs}}{dt} = -R_s i_{bs} + V_{bs} - V_{bl} \quad (2)$$

$$L_s \frac{di_{cs}}{dt} = -R_s i_{cs} + V_{cs} - V_{cl} \quad (3)$$

$$\frac{d}{dt} \left(\frac{1}{2} C V_{dc}^2(t) \right) = -[V_{as} i_{as} + V_{bs} i_{bs} + V_{cs} i_{cs}] - \frac{V_{dc}^2(t)}{R_c} \quad (4)$$

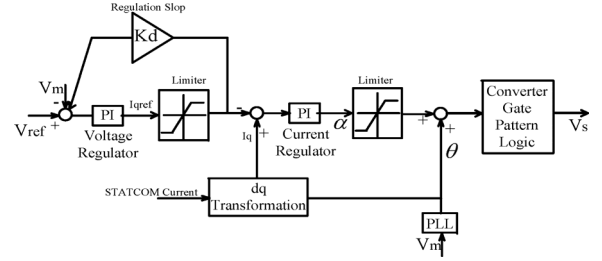


Fig. 2. Traditional STATCOM PI control block diagram.

By using the abc/dq transformation, the equations from (1) to (4) can be rewritten as

$$\frac{d}{dt} \begin{bmatrix} i_{ds} \\ i_{qs} \\ V_{dc} \end{bmatrix} = \begin{bmatrix} -\frac{R_s}{L_s} & \omega & \frac{K}{L_s} \cos \alpha \\ -\omega & -\frac{R_s}{L_s} & \frac{K}{L_s} \sin \alpha \\ -\frac{3K}{2C} \cos \alpha & -\frac{3K}{2C} \sin \alpha & -\frac{1}{R_c C} \end{bmatrix} \begin{bmatrix} i_{ds} \\ i_{qs} \\ V_{dc} \end{bmatrix} - \frac{1}{L_s} \begin{bmatrix} V_{dt} \\ V_{qt} \\ 0 \end{bmatrix} \quad (5)$$

where i_{ds} and i_{qs} are the d and q currents corresponding to i_{as} , i_{bs} , and i_{cs} ; K is a factor that relates the dc voltage to the peak phase-to-neutral voltage on the ac side; V_{dc} is the dc-side voltage; α is the phase angle at which the STATCOM output voltage leads the bus voltage; ω is the synchronously rotating angle speed of the voltage vector; and V_{dt} and V_{qt} represent the d and q axis voltage corresponding to V_{al} , V_{bl} , and V_{cl} . Since $V_{qt} = 0$, based on the instantaneous active and reactive power definition, (6) and (7) can be obtained as follows [23], [24]:

$$p_l = \frac{3}{2} V_{dt} i_{ds} \quad (6)$$

$$q_l = \frac{3}{2} V_{dt} i_{qs} \quad (7)$$

Based on the above equations, the traditional control strategy can be obtained, and the STATCOM control block diagram is shown in Fig. 2 [10], [11], [25].

As shown in Fig. 2, the phase-locked loop (PLL) provides the basic synchronizing signal which is the reference angle to the measurement system. Measured bus line voltage V_m is compared with the reference voltage V_{ref} , and the voltage regulator provides the required reactive reference current I_{qref} . The droop factor K_d is defined as the allowable voltage error at the rated reactive current flow through the STATCOM. The STATCOM reactive current I_q is compared with I_{qref} , and the output of the current regulator is the angle phase shift of the inverter voltage with regard to the system voltage. The limiter is the limit imposed on the value of control while considering the maximum reactive power capability of the STATCOM.

III. ADAPTIVE PI CONTROL FOR STATCOM

A. Concept of the Proposed Adaptive PI Control Method

The STATCOM with fixed PI control parameters may not reach the desired and acceptable response in the power system when the power system operating condition (e.g., loads or transmissions) changes. An adaptive PI control method is presented

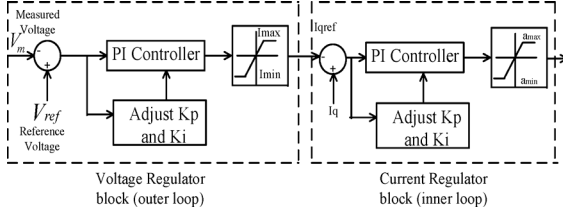


Fig. 3. Adaptive PI control block for STATCOM.

in this section in order to obtain the desired response and to avoid performing trial-and-error studies to find suitable parameters for PI controllers when a new STATCOM is installed in a power system. With this adaptive PI control method, the dynamical self-adjustment of PI control parameters can be realized.

An adaptive PI control block for STATCOM is shown in Fig. 3. In Fig. 3, the measured voltage $V_m(t)$ and the reference voltage $V_{ref}(t)$, and the q -axis reference current I_{qref} and the q -axis current I_q are in per-unit values. The proportional and integral parts of the voltage regulator gains are denoted by K_{p-V} and K_{i-V} , respectively. Similarly, the gains K_{p-I} and K_{i-I} represent the proportional and integral parts, respectively, of the current regulator. In this control system, the allowable voltage error K_d is set to 0. The K_{p-V} , K_{i-V} , K_{p-I} , and K_{i-I} can be set to an arbitrary initial value such as simply 1.0. One exemplary desired curve is an exponential curve in terms of the voltage growth, shown in Fig. 4, which is set as the reference voltage in the outer loop. Other curves may also be used than the depicted exponential curve as long as the measured voltage returns to the desired steady-state voltage in desired time duration. The process of the adaptive voltage-control method for STATCOM is described as follows.

- 1) The bus voltage $V_m(t)$ is measured in real time.
- 2) When the measured bus voltage over time $V_m(t) \neq V_{ss}$, the target steady-state voltage, which is set to 1.0 per unit (p.u.) in the discussion and examples, $V_m(t)$ is compared with V_{ss} . Based on the desired reference voltage curve, K_{p-V} and K_{i-V} are dynamically adjusted in order to make the measured voltage match the desired reference voltage, and the q -axis reference current I_{qref} can be obtained.
- 3) In the inner loop, I_{qref} is compared with the q -axis current I_q . Using the similar control method like the one for the outer loop, the parameters K_{p-I} and K_{i-I} can be adjusted based on the error. Then, a suitable angle can be found and eventually the dc voltage in STATCOM can be modified such that STATCOM provides the exact amount of reactive power injected into the system to keep the bus voltage at the desired value.

It should be noted that the current I_{max} and I_{min} and the angle α_{max} and α_{min} are the limits imposed with the consideration of the maximum reactive power generation capability of the STATCOM controlled in this manner. If one of the maximum or minimum limits is reached, the maximum capability of the STATCOM to inject reactive power has been reached. Certainly, as long as the STATCOM sizing has been appropriately studied during planning stages for inserting the STATCOM into the power system, the STATCOM should not reach its limit unexpectedly.

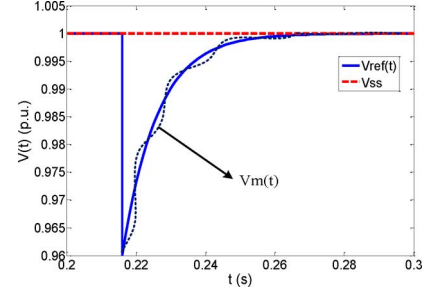


Fig. 4. Reference voltage curve.

B. Derivation of the Key Equations

Since the inner loop control is similar to the outer loop control, the mathematical method to automatically adjust PI controller gains in the outer loop is discussed in this section for illustrative purposes. A similar analysis can be applied to the inner loop.

Here, $V_{dl}(t)$ and $V_{ql}(t)$ can be computed with the d - q transformation

$$\begin{bmatrix} V_{dl}(t) \\ V_{ql}(t) \\ 0 \end{bmatrix} = \frac{2}{3} \begin{bmatrix} 1 & -\frac{1}{2} & -\frac{1}{2} \\ 0 & \frac{\sqrt{3}}{2} & -\frac{\sqrt{3}}{2} \\ \frac{1}{\sqrt{2}} & \frac{1}{\sqrt{2}} & \frac{1}{\sqrt{2}} \end{bmatrix} \begin{bmatrix} V_{al}(t) \\ V_{bl}(t) \\ V_{cl}(t) \end{bmatrix}. \quad (8)$$

Then, we have

$$V_m(t) = \sqrt{V_{dl}^2(t) + V_{ql}^2(t)}. \quad (9)$$

Based on $V_m(t)$, the reference voltage $V_{ref}(t)$ is set as

$$V_{ref}(t) = V_{ss} - (V_{ss} - V_m(t))e^{-\frac{t}{\tau}}. \quad (10)$$

In (10), V_{ss} is the target steady-state voltage, which is set to 1.0 p.u. in the discussion and examples; $V_m(t)$ is the measured voltage; $\tau = 0.01$ s. The curve in Fig. 4 is one examples of $V_{ref}(t)$.

If the system is operating in the normal condition, then $V_m(t) = 1$ p.u. and, thus, $V_{ref}(t) = 1$ p.u. This means that K_{p-V} and K_{i-V} will not change and the STATCOM will not inject or absorb any reactive power to maintain the voltage meeting the reference voltage. However, once there is a voltage disturbance in the power system, based on $V_{ref}(t) = V_{ss} - (V_{ss} - V_m(t))e^{-(t)/(\tau)}$, K_{p-V} and K_{i-V} will become adjustable and the STATCOM will provide reactive power to increase the voltage. Here, the error between $V_{ref}(t)$ and $V_m(t)$ is denoted by $\Delta V(t)$ when there is a disturbance in the power system. Based on the adaptive voltage-control model, at any arbitrary time instant t , the following equation can be obtained:

$$\Delta V(t)K_{p-V}(t) + K_{i-V}(t) \int_t^{t+T_s} \Delta V(t)dt = I_{qref}(t + T_s) \quad (11)$$

where T_s is the sample time, which is set to 2.5×10^{-5} s here as an example.

In this system, the discrete-time integrator block in place of the integrator block is used to create a purely discrete system, and the Forward-Euler method is used in the discrete-time integrator block. Therefore, the resulting expression for the output of the discrete-time integrator block at t is

$$y(t) = y(t - T_s) + K_{i_V}(t - T_s) \times T_s \times \Delta V(t - T_s) \quad (12)$$

where $y(t) = K_{i_V}(t) \int_t^{t+T_s} \Delta V(t) dt$; $y(t - T_s) = K_{i_V}(t - T_s) \int_{t-T_s}^t \Delta V(t - T_s) dt$.

Considering $y(t - T_s) = I_{qref}(t)$, we can rewrite (11) as follows:

$$\begin{aligned} & \Delta V(t) K_{p_V}(t) + K_{i_V}(t) \int_t^{t+T_s} \Delta V(t) dt \\ & - K_{i_V}(t - T_s) \int_{t-T_s}^t \Delta V(t - T_s) dt \\ & = I_{qref}(t + T_s) - I_{qref}(t). \end{aligned} \quad (13)$$

Over a very short time duration, we can consider $K_{i_V}(t) = K_{i_V}(t - T_s)$. Hence, (13) can be rewritten as

$$\Delta V(t) K_{p_V}(t) + K_{i_V}(t) \int_t^{t+T_s} A dt = I_{qref}(t + T_s) - I_{qref}(t) \quad (14)$$

where $A = \Delta V(t) - \Delta V(t - T_s)$.

Based on (12), if we can determine in ideal response the ratio $(I_{qref}(t + T_s) - I_{qref}(t))/(\Delta V(t))$ and the ideal ratio $(K_{i_V}(t))/(K_{p_V}(t))$, the desired $K_{p_V}(t)$ and $K_{i_V}(t)$ can be solved.

Assume at the ideal response, we have

$$I_{qref}(t + T_s) - I_{qref}(t) = R \times \Delta V(t). \quad (15)$$

Since the system is expected to be stable, without losing generality, we may assume that the bus voltage will come back to 1 p.u. in 5τ , where 5τ is the delay defined by users as shown in Fig. 4. Since $I_{qref}(t_0) = 0$ based on (15), (11) can be rewritten as

$$\Delta V(t_0) K_{p_V}(t_0) + K_{i_V}(t_0) \int_{t_0}^{t_0+5\tau} \Delta V(t) dt = R \times \Delta V(t_0) \quad (16)$$

where t_0 is the time that the system disturbance occurs.

Setting $K_{i_V}(t_0^-) = 0$, we then have

$$K_{p_V}(t_0) = R. \quad (17)$$

Setting $K_{p_V}(t_0^-) = 0$, we then have

$$K_{i_V}(t_0) = \frac{\Delta V(t_0) \times R}{\int_{t_0}^{t_0+5\tau} \Delta V(t) dt}. \quad (18)$$

Now, the ratio $m_V = (K_{i_V}(t_0))/(K_{p_V}(t_0))$ can be considered as the ideal ratio of the values of $K_{p_V}(t)$ and $K_{i_V}(t)$ after fault.

Thus, (15) can be rewritten as

$$I_{qref}(t + 5\tau) - I_{qref}(t) = k_V \times \Delta V(t_0). \quad (19)$$

Here, k_V can be considered as the steady and ideal ratio $(I_{qref}(t + T_s) - I_{qref}(t))/(\Delta V(t))$.

Based on the system bus capacity and the STATCOM rating, ΔV_{max} can be obtained, which means any voltage change greater than ΔV_{max} cannot come back to 1 p.u. Since we have $-1 \leq I_{qref}(t) \leq 1$, we have the following equation:

$$\begin{aligned} & \frac{\Delta V(t_0)}{\Delta V_{max}} = k_V \\ & \times \frac{\Delta V(t_0) K_{p_V}(t_0) + K_{i_V}(t_0) \int_{t_0}^{t_0+5\tau} \Delta V(t) dt}{R}. \end{aligned} \quad (20)$$

Based on (16), (19), and (20), k_V can be calculated by (21), shown at the bottom of the page.

In order to exactly calculate the PI controller gains based on (14), we can derive

$$\Delta V(t) K_{p_V}(t) + m_V K_{p_V}(t) \int_t^{t+T_s} A dt = k_V \times \Delta V(t). \quad (22)$$

Therefore, $K_{p_V}(t)$ and $K_{i_V}(t)$ can be computed by the following equations:

$$K_{p_V}(t) = \frac{k_V \times \Delta V(t)}{\left(\Delta V(t) + m_V \times \int_t^{t+T_s} A dt \right)} \quad (23)$$

$$K_{i_V}(t) = m_V \times K_{p_V}(t). \quad (24)$$

Therefore, based on (23) and (24), $K_{p_V}(t)$ and $K_{i_V}(t)$ can be adjusted dynamically.

Using a similar process, the following expressions for current regulator PI gains can be obtained:

$$K_{p_I}(t) = \frac{k_I \times \Delta I_q(t)}{\left(\Delta I_q(t) + m_I \times \int_t^{t+T_s} B dt \right)} \quad (25)$$

$$K_{i_I}(t) = m_I \times K_{p_I}(t) \quad (26)$$

where $\Delta I_q(t)$ is the error between I_{qref} and I_q , k_I is the steady and ideal ratio $(\alpha(t + T_s) - \alpha(t))/(\Delta I_q(t))$, and $\alpha(t)$ is the

$$k_V = \frac{R \times \Delta V(t_0)}{\left(K_{p_V}(t_0) \Delta V(t_0) + K_{i_V}(t_0) \int_{t_0}^{t_0+5\tau} \Delta V(t) dt \right) \times \Delta V_{max}}. \quad (21)$$

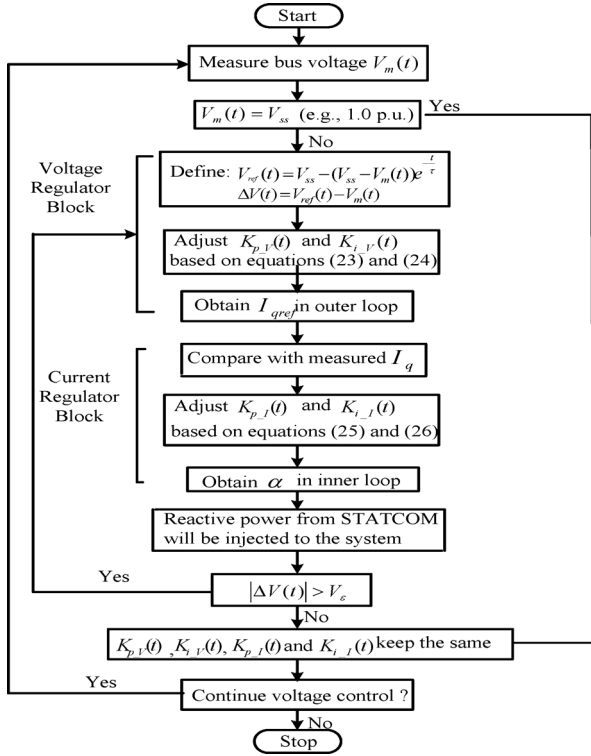


Fig. 5. Adaptive PI control algorithm flowchart.

angle of the phase shift of the inverter voltage with respect to the system voltage at time t ; m_I is the ideal ratio of the values of $K_{p-I}(t)$ and $K_{i-I}(t)$ after fault; and B is equal to $\Delta I_q(t) - \Delta I_q(t - T_S)$.

Note that the derivation from (10)–(26) is fully reversible so that it ensures that the measured voltage curve can follow the desired ideal response, as defined in (10).

C. Flowcharts of the Adaptive PI Control Procedure

Fig. 5 is an exemplary flowchart of the proposed adaptive PI control for STATCOM for the block diagram of Fig. 3.

The adaptive PI control process begins at Start. The bus voltage over time $V_m(t)$ is sampled according to a desired sampling rate. Then, $V_m(t)$ is compared with V_{ss} . If $V_m(t) = V_{ss}$, then there is no reason to change any of the identified parameters $K_{p-V}(t)$, $K_{i-V}(t)$, $K_{i-I}(t)$, and $K_{p-I}(t)$. The power system is running smoothly. On the other hand, if $V_m(t) \neq V_{ss}$, then adaptive PI control begins.

The measured voltage is compared with $V_{ref}(t)$, the reference voltage defined in (10). Then, $K_{p-V}(t)$ and $K_{i-V}(t)$ are adjusted in the voltage regulator block (outer loop) based on (23) and (24), which leads to an updated I_{qref} via a current limiter as shown in Fig. 3.

Then, the I_{qref} is compared with the measured q-current I_q . The control gains $K_{p-I}(t)$ and $K_{i-I}(t)$ are adjusted based on (25) and (26). Then, the phase angle α is determined and passed through a limiter for output, which essentially decides the reactive power output from the STATCOM.

Next, if $|\Delta V(t)|$ is not within a tolerance threshold V_ϵ , which is a very small value such as 0.0001 p.u., the voltage regu-

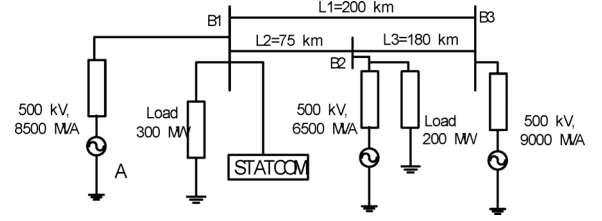


Fig. 6. Studied system.

lator block and current regulator blocks are re-entered until the change is less than the given threshold V_ϵ . Thus, the values for $K_{p-V}(t)$, $K_{i-V}(t)$, $K_{i-I}(t)$, and $K_{p-I}(t)$ are maintained.

If there is the need to continuously perform the voltage-control process, which is usually the case, then the process returns to the measured bus voltage. Otherwise, the voltage-control process stops (i.e., the STATCOM control is deactivated).

IV. SIMULATION RESULTS

A. System Data

In the system simulation diagram shown in Fig. 6, a ± 100 -MVAR STATCOM is implemented with a 48-pulse VSC and connected to a 500-kV bus. This is the standard sample STATCOM system in Matlab/Simulink library, and all machines used in the simulation are dynamical models [10]–[12]. Here, the attention is focused on the STATCOM control performance in bus voltage regulation mode. In the original model, the compensating reactive power injection and the regulation speed are mainly affected by PI controller parameters in the voltage regulator and the current regulator. The original control will be compared with the proposed adaptive PI control model.

Assume the steady-state voltage, $V_{ss} = 1.0$ p.u. In Sections IV-B, C, and F, a disturbance is assumed to cause a voltage drop at 0.2 s from 1.0 to 0.989 p.u. at the source (substation A). Here, the 0.989-p.u. voltage at substation A is the lowest voltage that the STATCOM system can support due to its capacity limit. The third simulation study in Subsection IV-D assumes a voltage drop from 1.0 to 0.991 under a changed load. The fourth simulation study in Subsection IV-E assumes a disturbance at 0.2 s, causing a voltage rise from 1.0 to 1.01 p.u. at substation A under a modified transmission network. In Subsection IV-F, a disturbance at 0.2 s causes a voltage decrease from 1.0 to 0.989 p.u. occurring at substation A. After that, line 1 is switched off at 0.25 s. In Subsection IV-G, a severe disturbance is assumed with a voltage sag of 60% of the rated voltage. When the fault clears, the voltage gets back to around 1.0 p.u.

In all simulation studies, the STATCOM immediately operates after the disturbance with the expectation of bringing the voltage back to 1.0 p.u. The proposed control and the original PI control are studied and compared.

B. Response of the Original Model

In the original model, $K_{p-V} = 12$, $K_{i-V} = 3000$, $K_{p-I} = 5$, $K_{i-I} = 40$. Here, we keep all of the parameters unchanged. The initial voltage source, shown in Fig. 6, is 1 p.u., with the

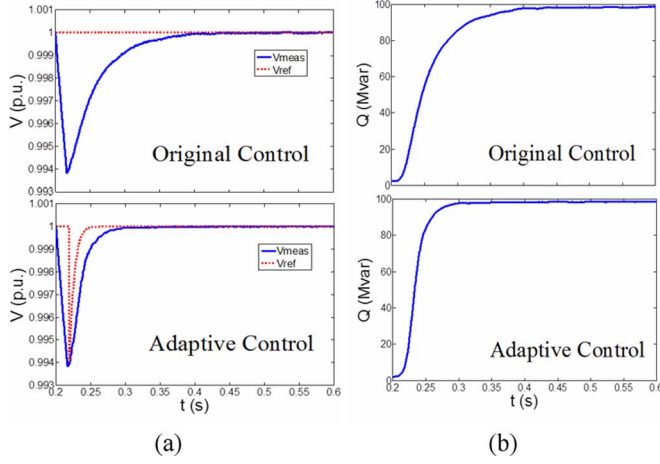


Fig. 7. Results of (a) voltages and (b) output reactive power using the same network and loads as in the original system.

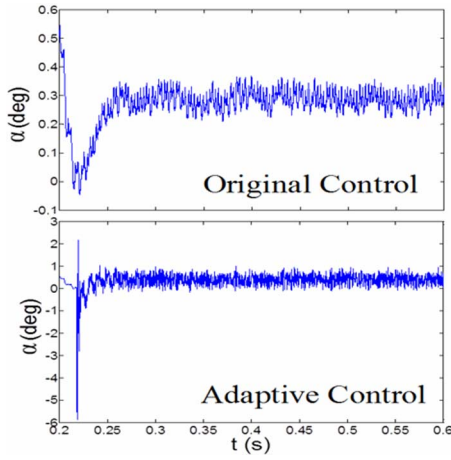


Fig. 8. Results of α using the same network and loads as in the original system.

voltage base being 500 kV. In this case, if we set $R = 1$, then we have the initial m_V calculated as $m_V = 770.8780$. Since, in this case, $\Delta V(t_0) = \Delta V_{\max}$ and $k_V = 84.7425$, based on (23)–(26), we have

$$K_{p-V}(t) = \frac{84.7425 \times \Delta V(t)}{\left(\Delta V(t) + 770.8780 \times \int_t^{t+T_s} A dt \right)} \quad (27)$$

$$K_{i-V}(t) = 770.8480 \times K_{p-V}(t) \quad (28)$$

$$K_{p-I}(t) = \frac{57.3260 \times \Delta I_q(t)}{\left(\Delta I_q(t) + 2.3775 \times \int_t^{t+T_s} B dt \right)} \quad (29)$$

$$K_{i-I}(t) = 2.3775 \times K_{p-I}(t). \quad (30)$$

Based on (27)–(30), the adaptive PI control system can be designed, and the results are shown in Figs. 7 and 8, respectively. Observations are summarized in Table I.

From the results, it is obvious that the adaptive PI control can achieve quicker response than the original one. The necessary reactive power amount is the same while the adaptive PI approach runs faster, as the voltage does.

Set $\omega t = \alpha + \theta$, where α is the output angle of the current regulator, and θ is the reference angle to the measurement system.

TABLE I
PERFORMANCE COMPARISON FOR THE ORIGINAL SYSTEM PARAMETERS

	Original Ctrl.	Adaptive Ctrl.
Lowest Voltage after disturbance	0.9938 p.u.	0.9938 p.u.
Time (sec) when $V=1.0$	0.4095 sec	0.2983 sec
Δt to reach $V=1.0$	0.2095 sec	0.0983 sec
Var Amount at steady state	97.76 MVar	97.65 MVar
Time to reach steady state Var	0.4095 sec	0.2983 sec

In the STATCOM, it is ωt that decides the control signal. Since θ is a very large value (varying between 0 to 2π), the ripples of α in the scale shown in Fig. 8 will not affect the final simulation results.

Note that there is a very slight difference of 0.12 MVar in the var amount at steady state in Table I, which should be caused by computational roundoff error. The reason is that the sensitivity of $d\text{Var}/dV$ is around 100 MVar/0.011 p.u. of voltage. For simplicity, we may assume that $\Delta\text{Var}/\Delta V$ sensitivity is a linear function. Thus, when the voltage error is 0.00001 p.u., ΔVar is 0.0909 MVar, which is in the same range as the 0.12-MVar mismatch. Thus, it is reasonable to conclude that the slight Var difference in Table I is due to roundoff error in the dynamic simulation which always gives tiny ripples beyond 5th digits even in the final steady state.

C. Change of PI Control Gains

In this scenario, the other system parameters remain unchanged while the PI controller gains for the original control are changed to $K_{p-V} = 1$, $K_{i-V} = 1$, $K_{p-I} = 1$, $K_{i-I} = 1$.

The dynamic control gains, which are independent of the initial values before the disturbance but depend on the postfault conditions, are given as

$$K_{p-V}(t) = \frac{80.1632 \times \Delta V(t)}{\left(\Delta V(t) + 732.3115 \times \int_t^{t+T_s} A dt \right)} \quad (31)$$

$$K_{i-V}(t) = 732.3115 \times K_{p-V}(t) \quad (32)$$

$$K_{p-I}(t) = \frac{47.4959 \times \Delta I_q(t)}{\left(\Delta I_q(t) + 1.8232 \times \int_t^{t+T_s} B dt \right)} \quad (33)$$

$$K_{i-I}(t) = 1.8232 \times K_{p-I}(t). \quad (34)$$

Based on (31)–(34), the adaptive PI control model can be designed, and the results are shown in Figs. 9 and 10, respectively.

From Fig. 9(a), it can be observed that when the PI control gains are changed to different values, the original control model cannot make the bus voltage get back to 1 p.u., and the STATCOM has poor response. The reactive power cannot be increased to a level to meet the need. However, with adaptive PI control, the STATCOM can respond to disturbance perfectly as desired, and the voltage can get back to 1 p.u. quickly within 0.1 s. Fig. 9(b) also shows that the reactive power injection cannot be continuously increased in the original control to support voltage, while the adaptive PI control performs as desired.

D. Change of Load

In this case, the original PI controller gains are kept, which means $K_{p-V} = 12$, $K_{i-V} = 3000$, $K_{p-I} = 5$ and $K_{i-I} = 40$.

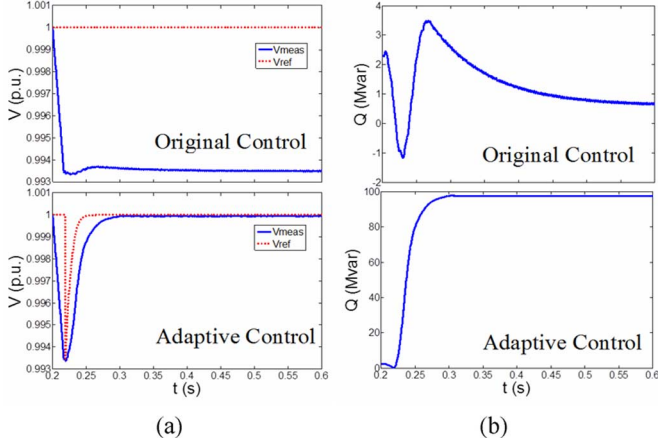


Fig. 9. Results of (a) voltages and (b) output reactive power with changed PI control gains.

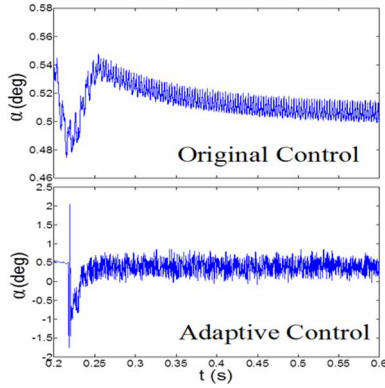


Fig. 10. Results of α with changed PI control gains.

However, the load at Bus B1 changes from 300 to 400 MW. In this case, we have the given dynamic control gains by

$$K_{p-V}(t) = \frac{93.3890 \times \Delta V(t)}{\left(\Delta V(t) + 187.5579 \times \int_t^{t+T_s} A dt \right)} \quad (35)$$

$$K_{i-V}(t) = 187.5579 \times K_{p-V}(t) \quad (36)$$

$$K_{p-I}(t) = \frac{8.1731 \times \Delta I_q(t)}{\left(\Delta I_q(t) + 13.1652 \times \int_t^{t+T_s} B dt \right)} \quad (37)$$

$$K_{i-I}(t) = 13.1652 \times K_{p-I}(t). \quad (38)$$

Based on (35)–(38), the adaptive PI control model can be designed for automatic reaction to a change in loads. The results are shown in Figs. 11 and 12. Table II shows a few key observations of the performance.

From the data shown in Table II and Fig. 11, it is obvious that the adaptive PI control can achieve a quicker response than the original one.

E. Change of Transmission Network

In this case, the PI controller gains remain unchanged, as in the original model. However, line 1 is switched off at 0.2 s to represent a different network which may correspond to scheduled transmission maintenance. Here, we have

$$K_{p-V}(t) = \frac{18.3245 \times \Delta V(t)}{\left(\Delta V(t) + 286.9512 \times \int_t^{t+T_s} A dt \right)} \quad (39)$$

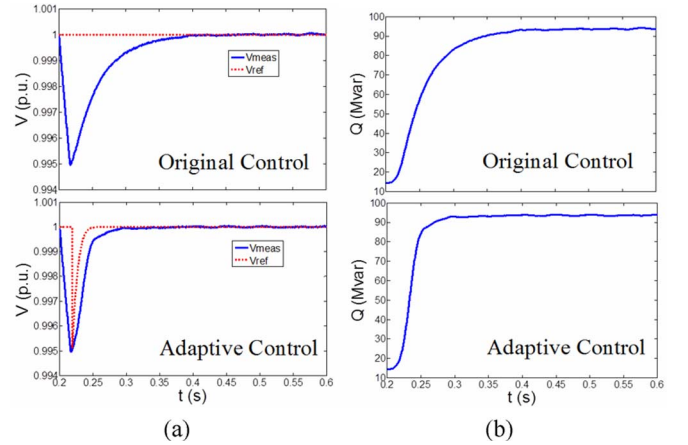


Fig. 11. Results of (a) voltages and (b) output reactive power with a change of load.

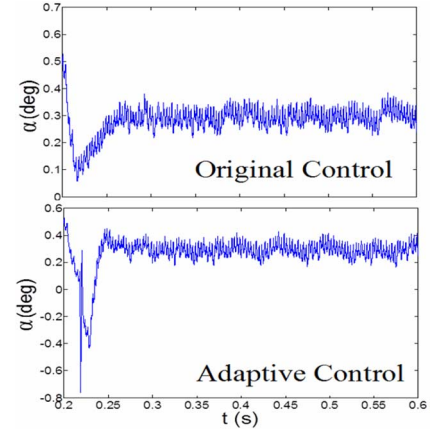


Fig. 12. Results of α with a change of load.

TABLE II
PERFORMANCE COMPARISON WITH A CHANGE OF LOAD

	Original Ctrl.	Adaptive Ctrl.
Lowest Voltage after disturbance	0.9949 p.u.	0.9949 p.u.
Time (sec) when V=1.0	0.4338 sec	0.3125 sec
Δt to reach V=1.0	0.2338 sec	0.1125 sec
Var Amount at steady state	93.08 MVar	92.72 MVar
Time to reach steady state VAR	0.4338 sec	0.3125 sec

$$K_{i-V}(t) = 286.9512 \times K_{p-V}(t) \quad (40)$$

$$K_{p-I}(t) = \frac{41.4360 \times \Delta I_q(t)}{\left(\Delta I_q(t) + 412.0153 \times \int_t^{t+T_s} B dt \right)} \quad (41)$$

$$K_{i-I}(t) = 412.0153 \times K_{p-I}(t). \quad (42)$$

Based on (39)–(42), the adaptive PI control model can be designed to automatically react to changes in the transmission network. The results are shown in Figs. 13 and 14. Key observations are summarized in Table III.

Note that the STATCOM absorbs VAR from the system in this case. Here, the disturbance is assumed to give a voltage rise at (substation A) from 1.0 to 1.01 p.u.; meanwhile, the system has a transmission line removed which tends to lower the voltages. The overall impact leads to a voltage rise to higher than 1.0 at the controlled bus in the steady state if the STATCOM is

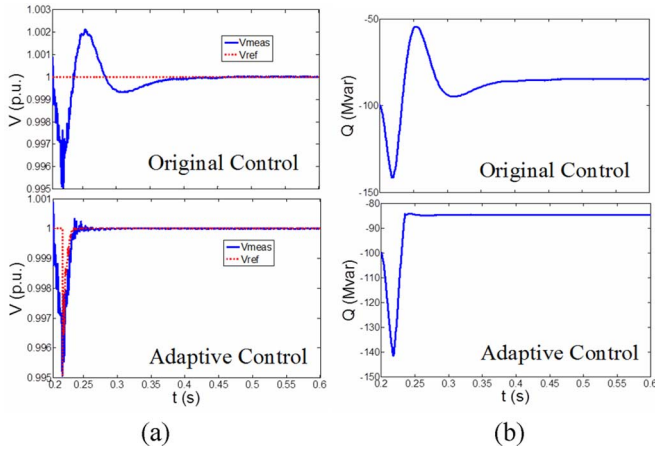


Fig. 13. Results of (a) voltages and (b) output reactive power with a change of transmission network.

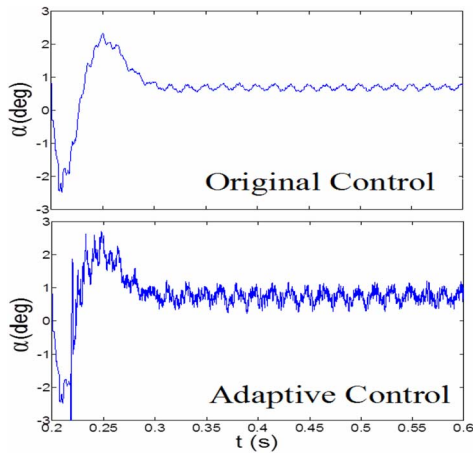


Fig. 14. Results of α with a change of transmission network.

TABLE III
PERFORMANCE COMPARISON WITH CHANGED TRANSMISSION

	Original Ctrl.	Adaptive Ctrl.
Lowest Voltage after disturbance	0.9954 p.u.	0.9954 p.u.
Time (sec) when $V=1.0$	0.4248 sec	0.2744 sec
Δt to reach $V=1.0$	0.2248 sec	0.0744 sec
Var Amount at steady state	-84.92 MVar	-85.02 MVar
Time to reach steady state Var	0.4248 sec	0.2744sec

not activated. Thus, the STATCOM needs to absorb VAR in the final steady state to reach 1.0 p.u. voltage at the controlled bus. Also note that the initial transients immediately after 0.2 s lead to an overabsorption by the STATCOM, while the adaptive PI control gives a much smoother and quicker response, as shown in Fig. 13.

F. Two Consecutive Disturbances

In this case, a disturbance at 0.2 s causes a voltage decrease from 1.0 to 0.989 p.u. and it occurs at substation A. After that, line 1 is switched off at 0.25 s.

The results are shown in Figs. 15 and 16. From Fig. 15, it is apparent that the adaptive PI control can achieve much quicker response than the original one, which makes the system voltage

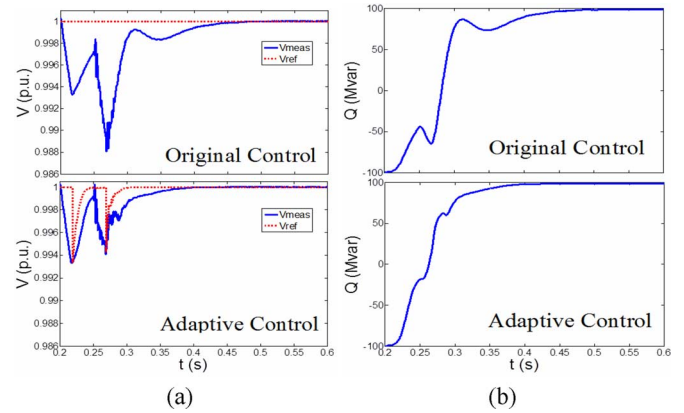


Fig. 15. Results of (a) voltages and (b) output reactive power with two consecutive disturbances.

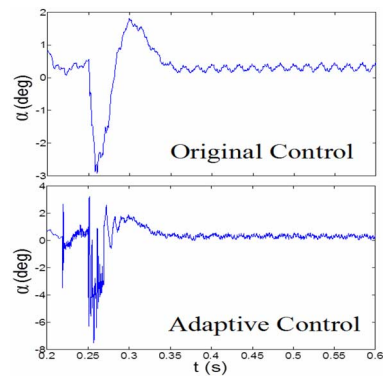


Fig. 16. Results of α with two consecutive disturbances.

drop much less than the original control during the second disturbance. Note in Fig. 15(a) that the largest voltage drop during the second disturbance event (starting at 0.25 s) with the original control is 0.012 p.u., while it is 0.006 p.u. with the proposed adaptive control. Therefore, the system is more robust in responding to consecutive disturbances with adaptive PI control.

G. Severe Disturbance

In this case, a severe disturbance at 0.2 s causes a voltage decrease from 1.0 to 0.6 p.u. and it occurs at substation A. After that, the disturbance is cleared at 0.25 s. The results are shown in Figs. 17 and 18. Due to the limit of STATCOM capacity, the voltage cannot get back to 1 p.u. after the severe voltage drop to 0.6 p.u. After the disturbance is cleared at 0.25 s, the voltage goes back to around 1.0 p.u. As shown in Fig. 17(a) and the two insets, the adaptive PI control can bring the voltage back to 1.0 p.u. much quicker and smoother than the original one. More important, the Q curve in the adaptive control ($Q^{\max} = 40$ MVar) is much less than the Q in the original control ($Q^{\max} = 118$ MVar).

H. Summary of the Simulation Study

From the aforementioned six case studies shown in Subsections B–G, it is evident that the adaptive PI control can achieve faster and more consistent response than the original one. The response time and the curve of the proposed

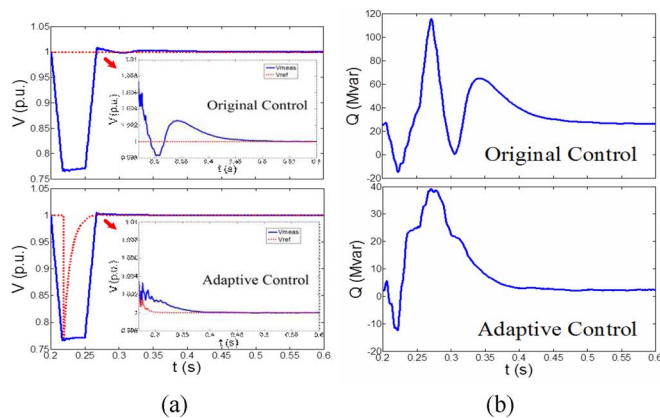


Fig. 17. Results of (a) voltages and (b) output reactive power in a severe disturbance.

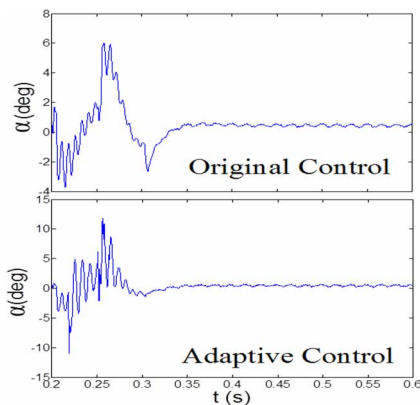


Fig. 18. Results of α in a severe disturbance.

adaptive PI control are almost identical under various conditions, such as a change of (initial) control gains, a change of load, a change of network topology, consecutive disturbances, and a severe disturbance. In contrast, the response curve of the original control model varies greatly under a change of system operating condition and worse, may not correct the voltage to the expected value.

The advantage of the proposed adaptive PI control approach is expected because the control gains are dynamically and autonomously adjusted during the voltage correction process; therefore, the desired performance can be achieved.

V. CONCLUSION AND FUTURE WORK

In the literature, various STATCOM control methods have been discussed including many applications of PI controllers. However, these previous works obtain the PI gains via a trial-and-error approach or extensive studies with a tradeoff of performance and applicability. Hence, control parameters for the optimal performance at a given operating point may not always be effective at a different operating point.

To address the challenge, this paper proposes a new control model based on adaptive PI control, which can self-adjust the control gains dynamically during disturbances so that the performance always matches a desired response, regardless

of the change of operating condition. Since the adjustment is autonomous, this gives the “plug-and-play” capability for STATCOM operation.

In the simulation study, the proposed adaptive PI control for STATCOM is compared with the conventional STATCOM control with pretuned fixed PI gains to verify the advantages of the proposed method. The results show that the adaptive PI control gives consistently excellent performance under various operating conditions, such as different initial control gains, different load levels, change of the transmission network, consecutive disturbances, and a severe disturbance. In contrast, the conventional STATCOM control with fixed PI gains has acceptable performance in the original system, but may not perform as efficient as the proposed control method when there is a change of system conditions.

Future work may lie in the investigation of multiple STATCOMs since the interaction among different STATCOMs may affect each other. Also, the extension to other power system control problems can be explored.

REFERENCES

- [1] F. Li, J. D. Kueck, D. T. Rzy, and T. King, “A preliminary analysis of the economics of using distributed energy as a source of reactive power supply,” Oak Ridge, TN, USA, First Quart. Rep. Fiscal Year, Apr. 2006, Oak Ridge Nat. Lab.
- [2] A. Jain, K. Joshi, A. Behal, and N. Mohan, “Voltage regulation with STATCOMs: Modeling, control and results,” *IEEE Trans. Power Del.*, vol. 21, no. 2, pp. 726–735, Apr. 2006.
- [3] D. Soto and R. Pena, “Nonlinear control strategies for cascaded multilevel STATCOMs,” *IEEE Trans. Power Del.*, vol. 19, no. 4, pp. 1919–1927, Oct. 2004.
- [4] F. Liu, S. Mei, Q. Lu, Y. Ni, F. F. Wu, and A. Yokoyama, “The nonlinear internal control of STATCOM: Theory and application,” *Int. J. Elect. Power Energy Syst.*, vol. 25, no. 6, pp. 421–430, 2003.
- [5] C. Hochgraf and R. H. Lasseter, “STATCOM controls for operation with unbalanced voltage,” *IEEE Trans. Power Del.*, vol. 13, no. 2, pp. 538–544, Apr. 1998.
- [6] G. E. Valdarannma, P. Mattavalli, and A. M. Stankonic, “Reactive power and unbalance compensation using STATCOM with dissipativity based control,” *IEEE Trans. Control Syst. Technol.*, vol. 19, no. 5, pp. 598–608, Sep. 2001.
- [7] H. F. Wang, “Phillips-Heffron model of power systems installed with STATCOM and applications,” *Proc. Inst. Elect. Eng., Gen. Transm. Distrib.*, vol. 146, no. 5, pp. 521–527, Sep. 1999.
- [8] H. F. Wang, “Applications of damping torque analysis to statcom control,” *Int. J. Elect. Power Energy Syst.*, vol. 22, pp. 197–204, 2000.
- [9] Y. Han, Y. O. Lee, and C. C. Chung, “Modified non-linear damping of internal dynamics via feedback linearisation for static synchronous compensator,” *IET Gen. Transm. Distrib.*, vol. 5, no. 9, pp. 930–940, 2011.
- [10] A. H. Norouzi and A. M. Sharaf, “Two control schemes to enhance the dynamic performance of the STATCOM and SSSC,” *IEEE Trans. Power Del.*, vol. 20, no. 1, pp. 435–442, Jan. 2005.
- [11] M. S. E. Moursi and A. M. Sharaf, “Novel controllers for the 48-pulse VSC STATCOM and SSSC for voltage regulation and reactive power compensation,” *IEEE Trans. Power Syst.*, vol. 20, no. 4, pp. 1985–1997, Nov. 2005.
- [12] Matlab & Simulink, GTO-based STATCOM Dec. 2013. [Online]. Available: <http://www.mathworks.com/help/physmod/sps/powersys/ug/gto-based-statcom.html>, Feb. 2012
- [13] H. Li, F. Li, J. D. Kueck, and D. T. Rzy, “Adaptive voltage control with distributed energy resources: Algorithm, theoretical analysis, simulation and field test verification,” *IEEE Trans. Power Syst.*, vol. 25, no. 3, pp. 1638–1647, Aug. 2010.
- [14] H. Li, F. Li, Y. Xu, D. T. Rzy, and S. Adhikari, “Autonomous and adaptive voltage control using multiple distributed energy resources,” *IEEE Trans. Power Syst.*, vol. 28, no. 2, pp. 718–730, May 2013.
- [15] P. Rao, M. L. Crow, and Z. Yang, “STATCOM control for power system voltage control applications,” *IEEE Trans. Power Del.*, vol. 15, no. 4, pp. 1311–1317, Oct. 2000.

- [16] W. L. Chen and Y. Y. Hsu, "Controller design for an induction generator driven by a variable speed wind turbine," *IEEE Trans. Energy Convers.*, vol. 21, no. 3, pp. 625–635, Sep. 2006.
- [17] K. Wang and M. L. Crow, "Power system voltage regulation via STATCOM internal nonlinear control," *IEEE Trans. Power Syst.*, vol. 26, no. 3, pp. 1252–1262, Aug. 2011.
- [18] V. Spitsa, A. Alexandrovitz, and E. Zeheb, "Design of a robust state feedback controller for a STATCOM using a zero set concept," *IEEE Trans. Power Del.*, vol. 25, no. 1, pp. 456–467, Jan. 2010.
- [19] A. Luo, C. Tang, Z. Shuai, J. Tang, X. Y. Xu, and D. Chen, "Fuzzy-PI-based direct-output-voltage control strategy for the STATCOM used in utility distribution systems," *IEEE Trans. Ind. Electron.*, vol. 56, no. 1, pp. 2401–2411, Jul. 2009.
- [20] A. H. M. A. Rahim, E. P. Nowicki, and J. M. Bakhshwain, "Fuzzy STATCOM control strategies for power system stabilization," in *Proc. ICGST Int. J. Autom. Control Syst. Eng.*, Feb. 2006, pp. 41–48.
- [21] L. O. Mak, Y. X. Ni, and C. M. Shen, "STATCOM with fuzzy controllers for interconnected power systems," *Elect. Power Syst. Res.*, vol. 55, pp. 87–95, 2000.
- [22] C.-H. Liu and Y.-Y. Hsu, "Design of a self-tuning PI controller for a STATCOM using particle swarm optimization," *IEEE Trans. Ind. Electron.*, vol. 57, no. 2, pp. 702–715, Feb. 2010.
- [23] C. Schauder and H. Mehta, "Vector analysis and control of the advanced static VAR compensators," *Proc. Inst. Elect. Eng., Gen., Transm., Distrib.*, vol. 140, no. 4, pp. 299–306, Jul. 1993.
- [24] I. Papic, P. Zunko, and D. Povh, "Basic control of unified power flow controller," *IEEE Trans. Power Syst.*, vol. 12, no. 4, pp. 1734–1739, Nov. 1997.
- [25] K. K. Sen, "Static synchronous compensator—Theory, modeling and applications," presented at the IEEE Power Eng. Soc. Winter Meeting, Edmonton, AB, Canada, Jan. 1999.



Yao Xu (S'11) received the B.S. and M.S. degrees in electrical engineering from Changsha University of Science and Technology, China, in 2006 and 2009, respectively, and is currently pursuing the Ph.D. degree at The University of Tennessee, Knoxville, TN, USA.

Her research interests include utility application of power electronics, power system control, power markets, and renewable energy integration.

Ms. Xu received the Min Kao Graduate Fellowship in Electrical Engineering.



Fangxing Li (S'98–M'01–SM'05), also known as Fran Li, received the B.S.E.E. and M.S.E.E. degrees from Southeast University, Nanjing, China, in 1994 and 1997, respectively, and the Ph.D. degree from Virginia Polytechnic Institute and State University, Blacksburg, VA, USA, in 2001.

Currently, he is an Associate Professor at The University of Tennessee (UT), Knoxville, TN, USA. His research interests include renewable energy integration, power markets, power system control, and power system computing.

Dr. Li is a registered P.E. in North Carolina, an Associate Editor of IEEE TRANSACTIONS ON SUSTAINABLE ENERGY, and a Fellow of IET.